Electronic Supplementary Material (ESI) for Sustainable Energy & Fuels.

Single Site Catalyst Supported in Mesoporous UiO-66 for Catalytic Conversion of Carbon Dioxide to Formate

Maureen Gumbo, [a,b] Edward Ocansey,[b] Banothile C.E. Makhubela,[b] Francoise M. Amombo Noa,[c] Lars Öhrström,[c] Obieda S. Mudraj,[d] and Gift Mehlana*[,a]

[a] Department of Chemical Sciences, Faculty of Science and Technology, Midlands State University, Private Bag 9055, Senga Road, Gweru, Zimbabwe

[b]Research Centre for Synthesis and Catalysis, Department of Chemical Sciences, University of Johannesburg, Auckland Park Kingsway Campus, Auckland Park, 2006, South Africa

[c]Chalmers University of Technology, Department of Chemistry and Chemical Engineering, SE-412 96, Göteborg, Sweden

[d]Materials Discovery Research Unit, Advanced Research Centre, Royal Scientific Society, Amman 11941, Jordan

E-mail: mehlanag@staff.msu.ac.zw

Estimated defects calculation.

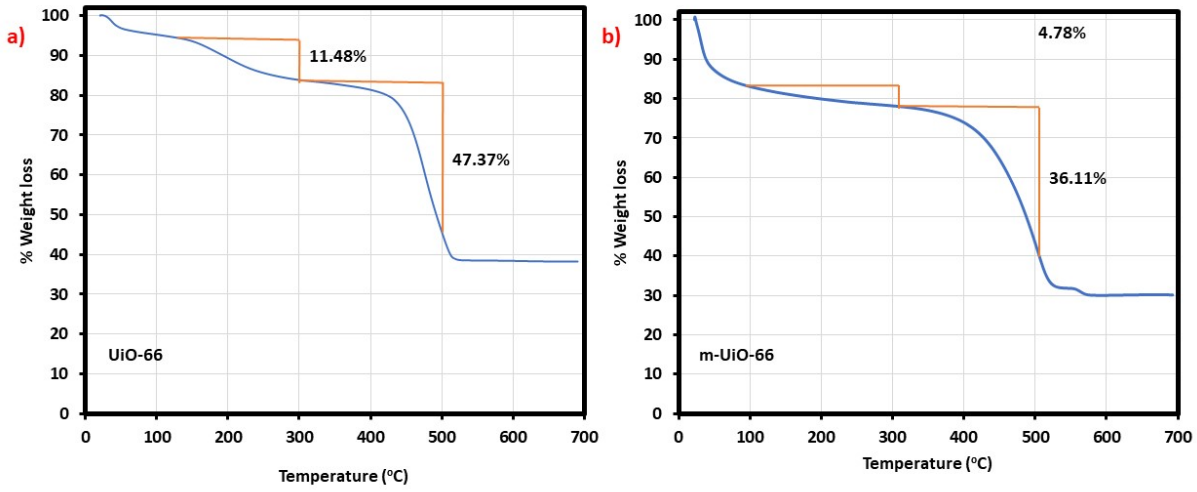

Figure S1. TGA analysis of, (a) Pristine UiO-66, and (b) Mesoporous m-UiO-66 in defects calculations.

Thermal decomposition of UiO-66, $Zr_6O_4(OH)_4(BDC)_6$ results in the loss of volatile substances and the organic linkers to yield ZrO_2. Pristine UiO-66 showed larger weight loss after 400 °C as compared to defective m-UiO-66. Weight loss below 100 °C was attributed to moisture and was not included in the calculation. The total weight loss in wt.% between 100 °C (linker-containing

phase) and 500 °C (ligands are decomposed) were 50.87% and 40.89% for pristine UiO-66 and mesoporous m-UiO-66 respectively.

Molecular weight of pristine UiO-66, $(Zr_6O_4(OH)_4(BDC)_6)$ = 1664.04 $gmol^{-1}$

Molecular weight of $(ZrO_2)_6$ = 739.32 $gmol^{-1}$

Expected % weight loss of linkers in pristine UiO-66 = (1664.04 - 739.32)/1664.04 = 55.6%

Experimental % weight loss of linkers in pristine UiO-66: (95.24 - 44. 37)/95.24 = 53.4%

Experimental % weight loss of linkers defective m-UiO-66: (82.97 - 42. 08)/82.97 = 49.3%

The theoretical loss of the linker was calculated as follows:

If UiO-66 lost 1 linker the formula becomes $Zr_6O_4(OH)_4(BDC)_5$ with molecular weight of 1499.92 $gmol^{-1}$

Estimated % weight loss in defective UiO-66 will be; (1499.92 - 739.32)/1499.92 = 51.2 %

Therefore, we can estimate that almost 1 linker in the asymmetric unit is missing in defective m-UiO-66 resulting in hierarchical mesoporous m-UiO-66.

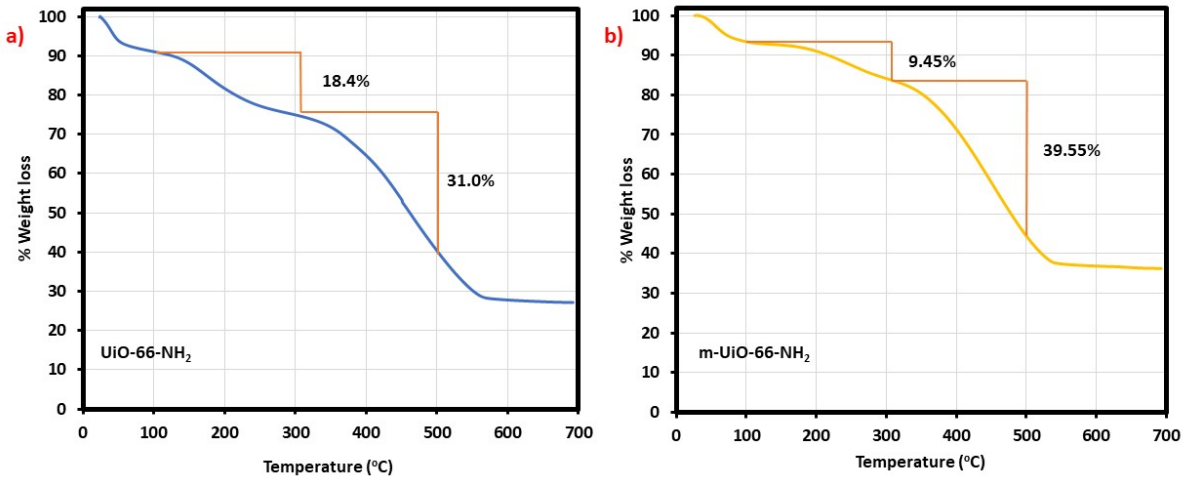

Figure S2. TGA analysis of, (a) Pristine UiO-66-NH_2, and (b) Mesoporous m-UiO-66-NH_2 in defects calculations.

Molecular weight of pristine UiO-66-NH_2, $(Zr_6O_4(OH)_4(BDC)_6)$ = 1754.1 $gmol^{-1}$

Molecular weight of $(ZrO_2)_6$ = 739.32 $gmol^{-1}$

Expected % weight loss of linkers in pristine UiO-66-NH_2= (1754.1 - 739.32)/ 1754.1 = 57.9%

Experimental % weight loss of linkers in pristine UiO-66-NH_2: (90.96 - 39. 69)/95.24 = 56.1%

Experimental % weight loss of linkers defective m-UiO-66-NH_2: (93.36 – 43.96)/93.36 = 52.9%

The theoretical loss of the linker was calculated as follows:

If UiO-66 lost 1 linker the formula becomes $Zr_6O_4(OH)_4(BDC\text{-}NH_2)_5$ with molecular weight of 1574.97 $gmol^{-1}$

Estimated % weight loss in defective m-UiO-66-NH_2 will be; (1574.97 - 739.32)/1574.97 = 53.1 %

Therefore, we can estimate that almost 1 linker in the asymmetric unit is missing in defective UiO-66-NH_2 resulting in hierarchical mesoporous m-UiO-66-NH_2.

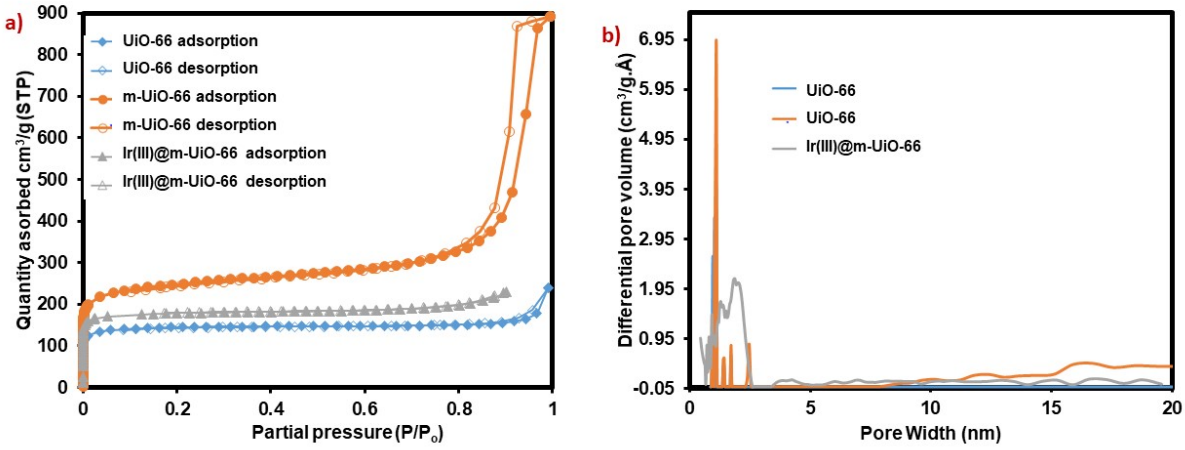

Figure S3. (a) Adsorption and desorption of UiO-66 and its derivatives at 77K. (b) Pore size analysis distribution of UiO-66 and its derivatives

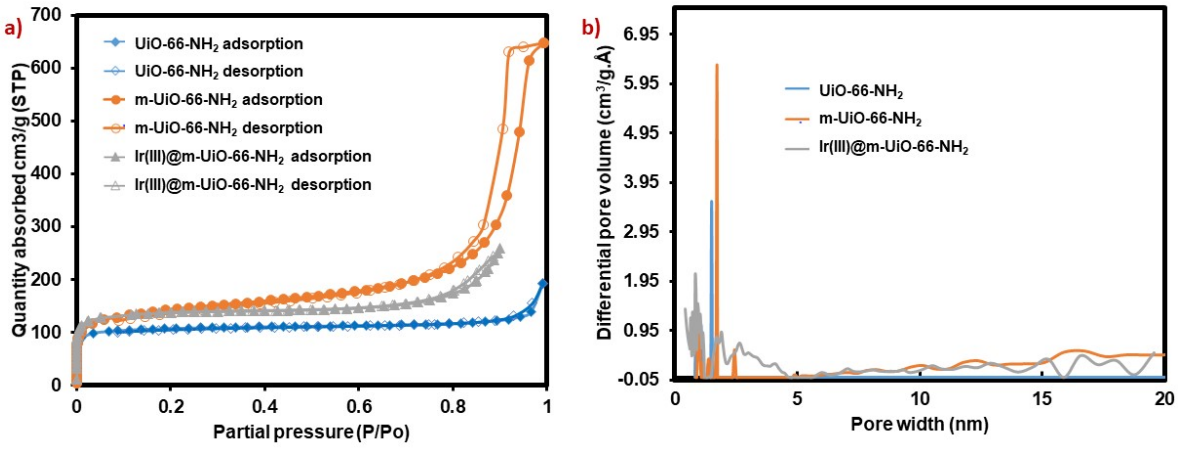

Figure S4. (a) Adsorption and desorption UiO-66-NH_2 and its derivatives at 77K. (b) Pore size analysis distribution of UiO-66-NH_2 and its derivatives

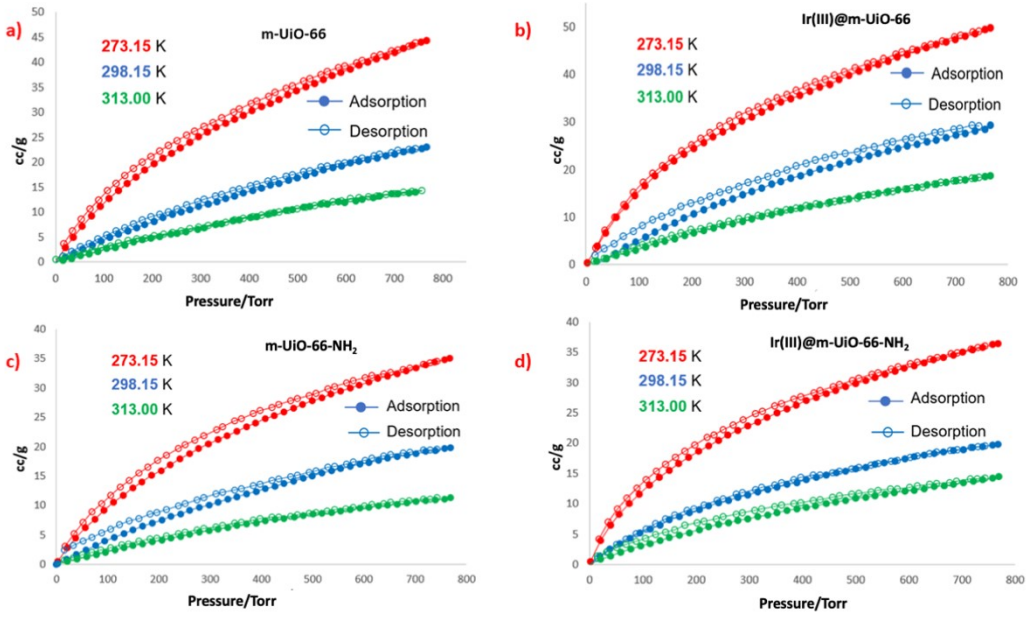

Figure S5. CO_2 sorption studies of, (a) m-UiO-66, (b) Ir(III)@m-UiO-66, (c) m-UiO-66-NH_2 and (d) Ir(III)@m-UiO-66-NH_2.

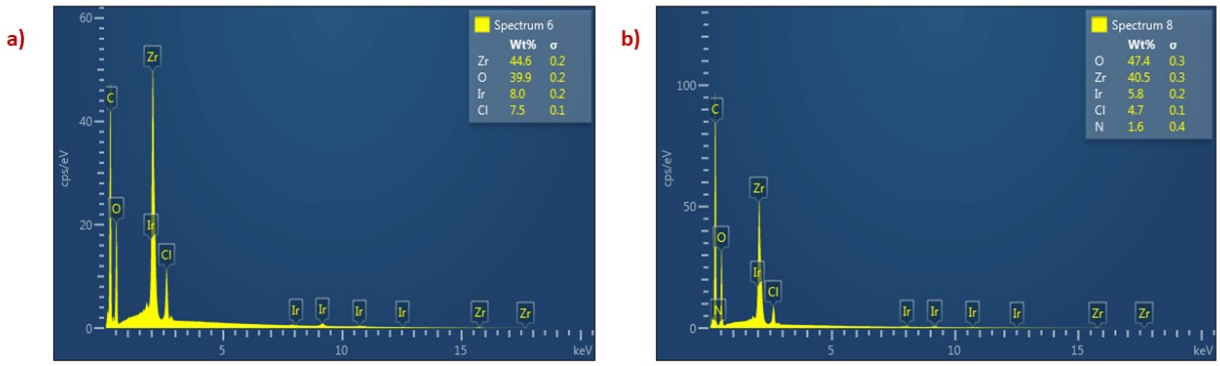

Figure S6. EDX spectrum of, (a) Ir(III)@m-UiO-66 and, (b) Ir(III)@m-UiO-66-NH_2.

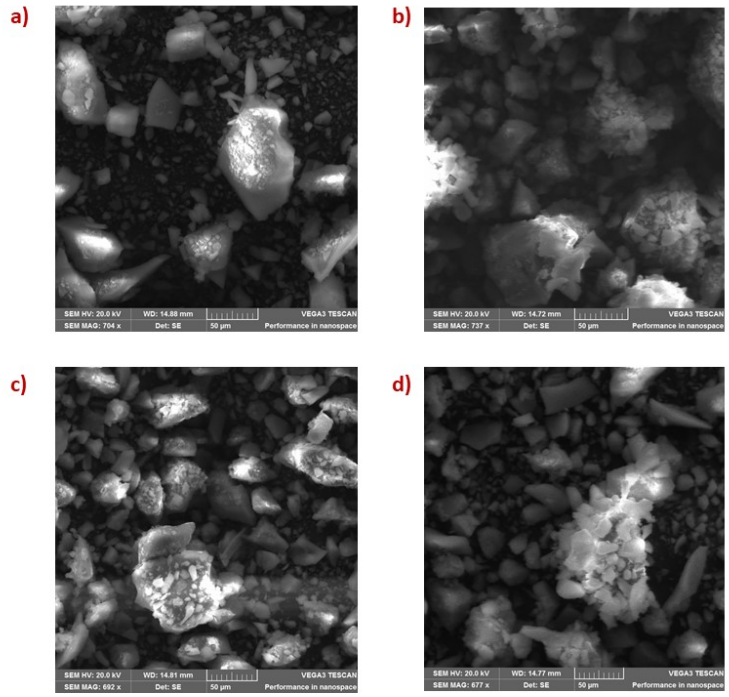

Figure S7. SEM images of (a) m-UiO-66, (b) m-UiO6-6-NH_2, (c) Ir(III)@m-UiO-66, and (d) Ir(III)@m-UiO-66-NH_2.

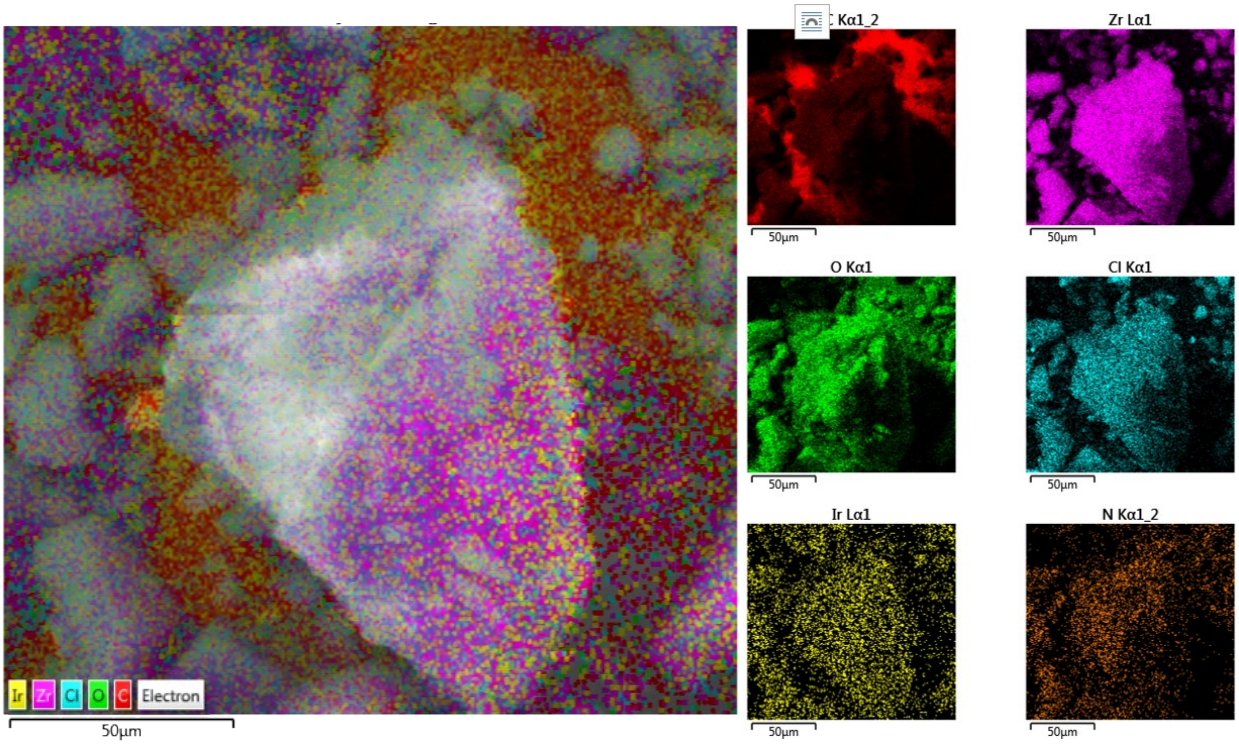

Figure S8. Elementary mapping of Ir(III)@m-UiO-66-NH_2.

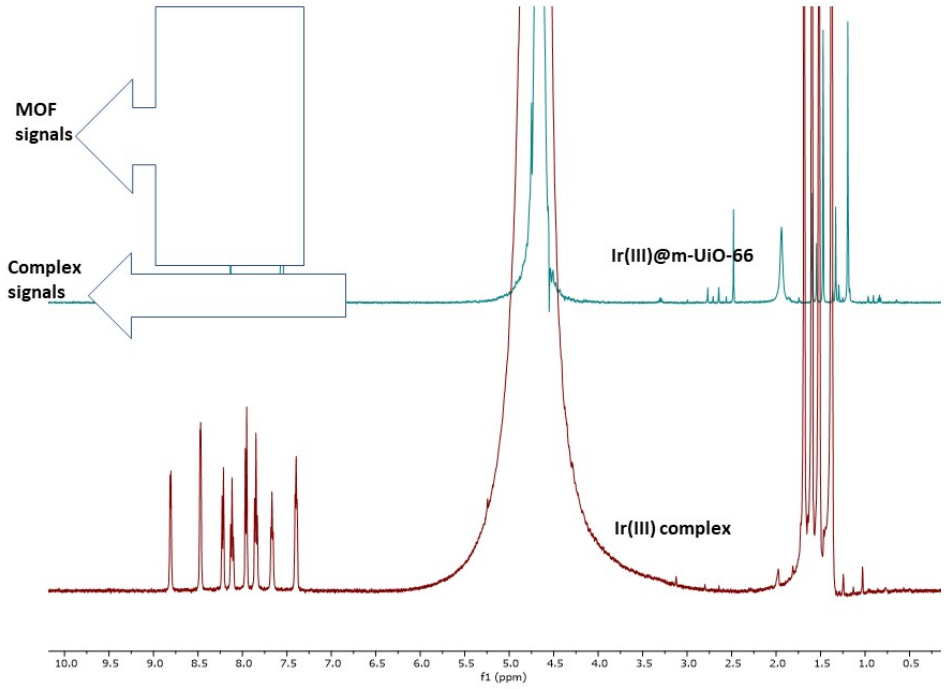

Figure S9. ^{1}H NMR analysis of Ir(III) complex and Ir(III)@m-UiO-66.

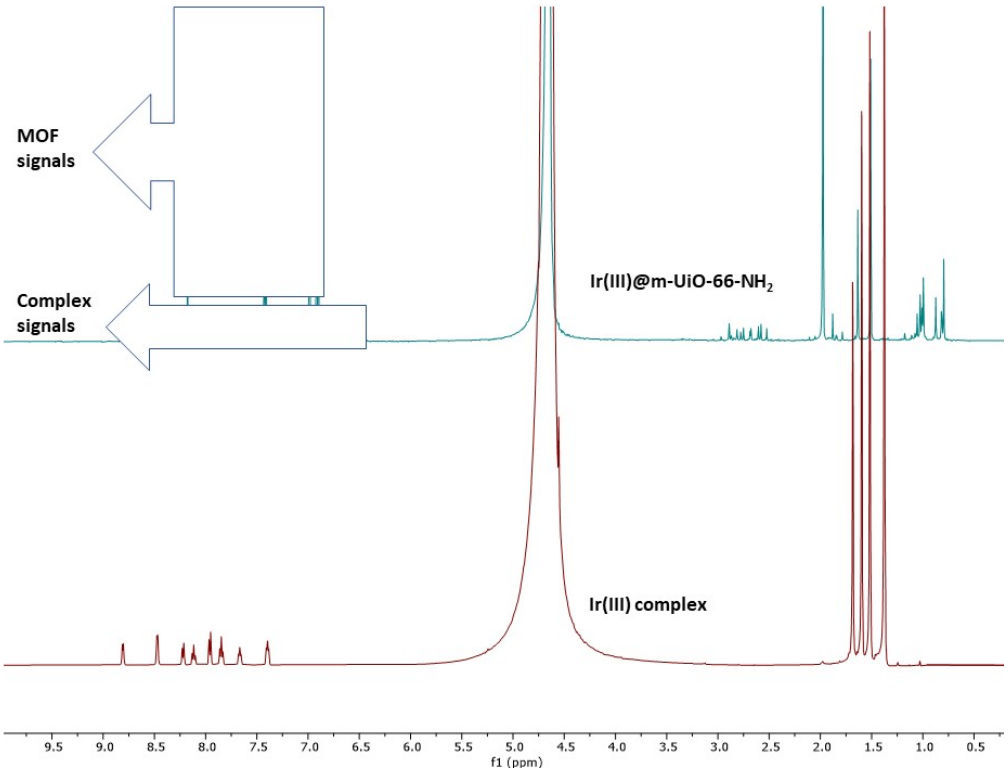

Figure S10: ^{1}H NMR analysis of Ir(III) complex and Ir(III)@m-UiO-66-NH_2.

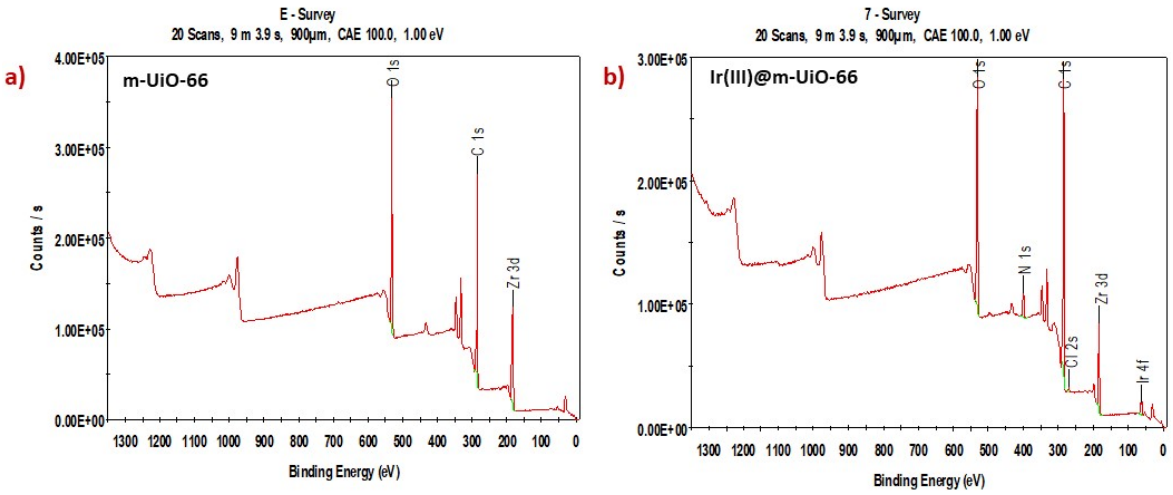

Figure S11. XPS spectra of m-UiO-66 and Ir(III)@m-UiO-66.

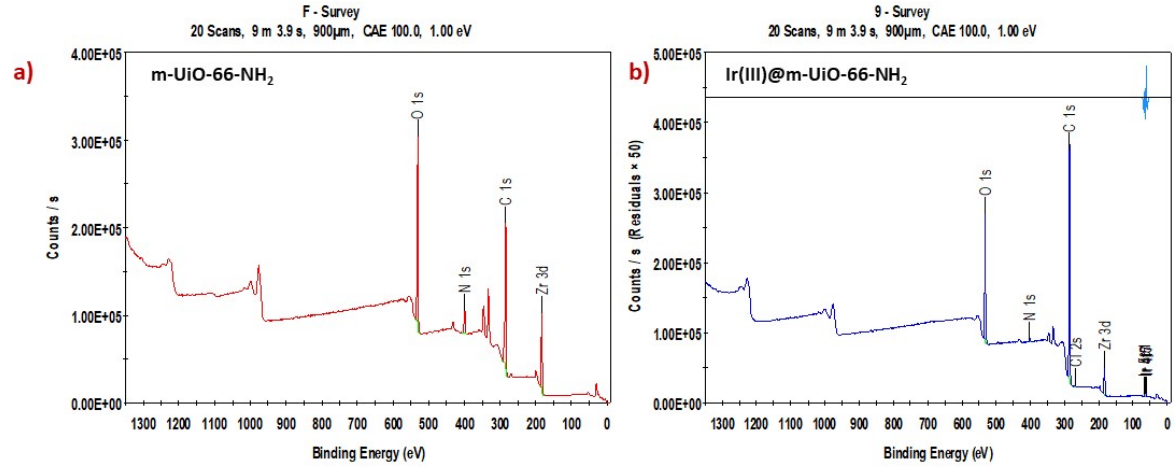

Figure S12. XPS spectra of m-UiO-66-NH_2 and Ir(III)@m-UiO-66-NH_2.

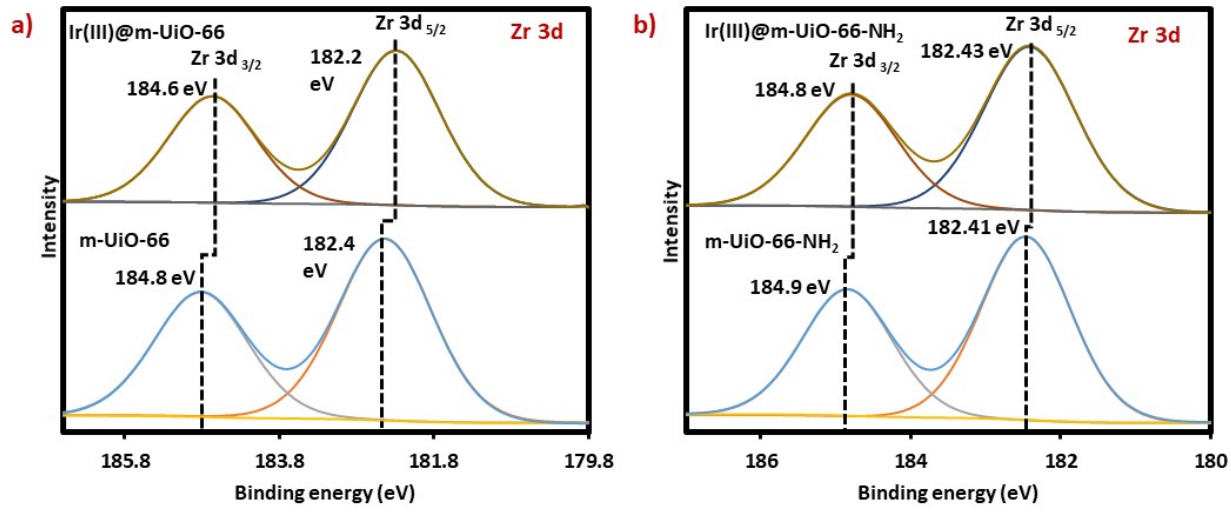

Figure S13. XPS analysis of Zr 3d in (a) Ir(III)@m-UiO-66 and (b) Ir(III)@m-UiO-66-NH_2.

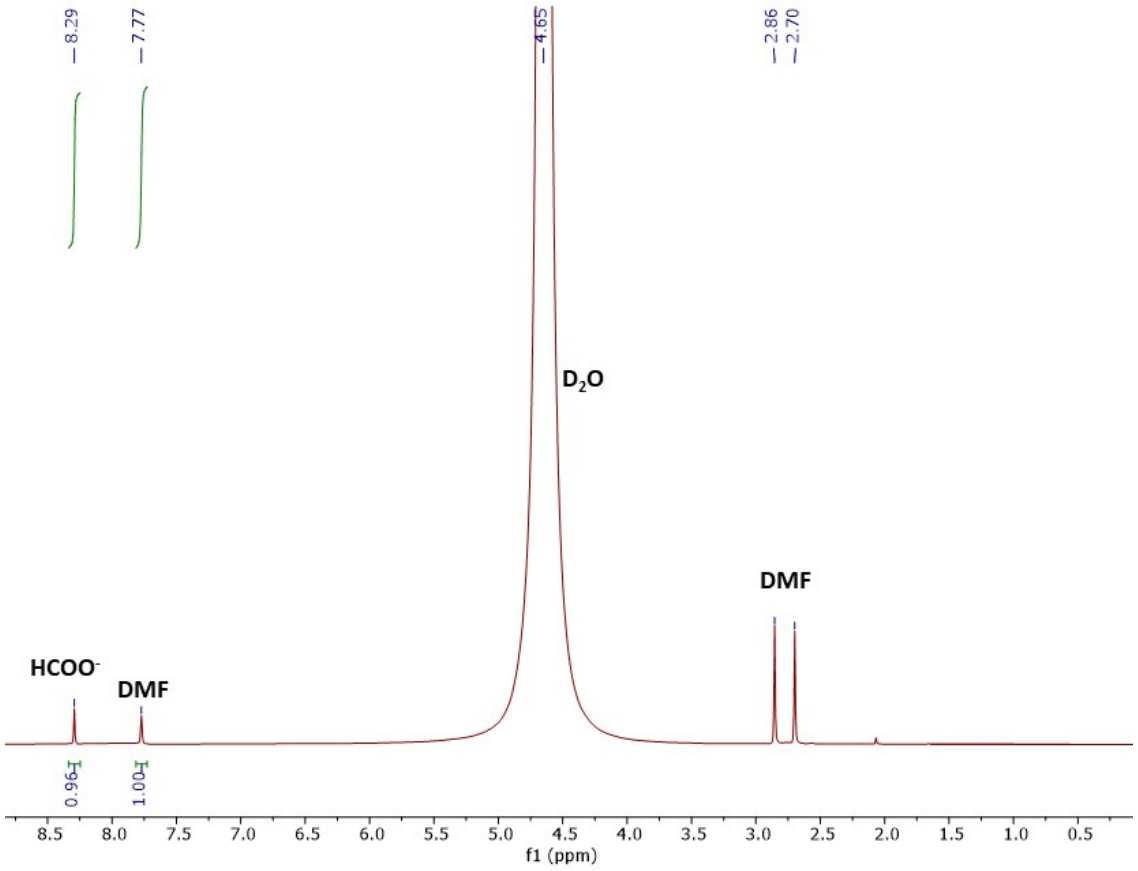

Figure S14. ^{1}H NMR analysis of formate detection and quantification.

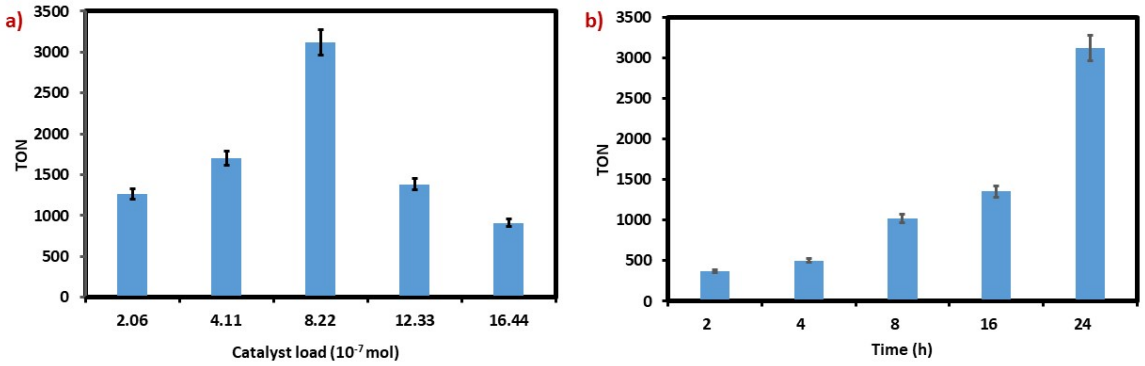

Figure S15. Catalysis optimisation studies conditions, 10 mL of water and 3.55 mmol of base (1/4 H_2:CO_2 total pressure 50 bar), time 24 h, temperature; 140 °C (a) catalyst load studies and, (b) time studies with 8 x 10^{-7} moles of catalyst.

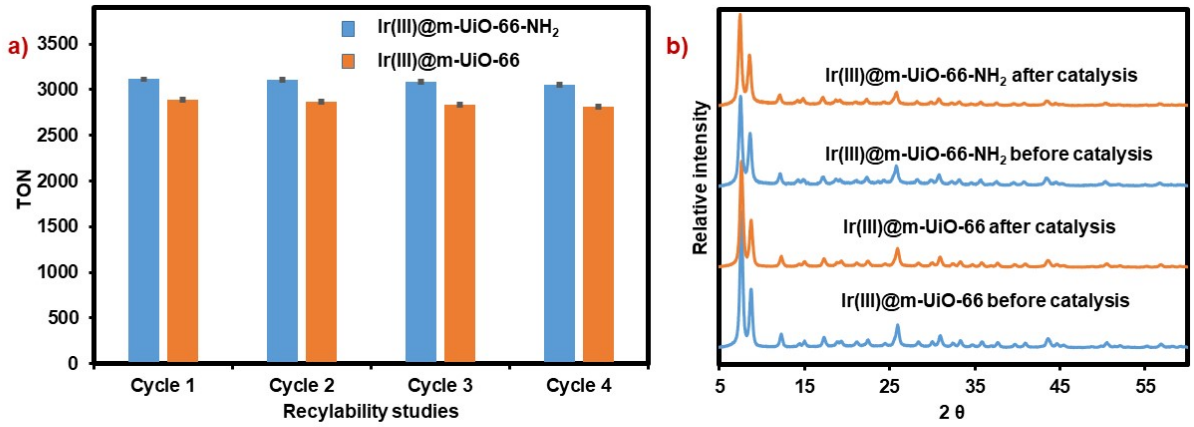

Figure S16. (a) Recyclability studies, (b) PXRD of recovered material after catalysis.

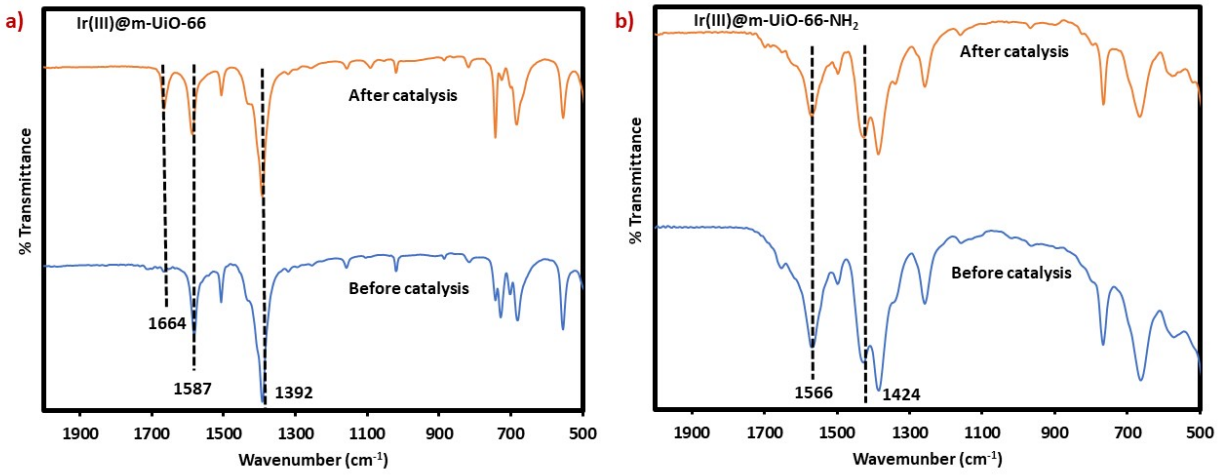

Figure S17. FTIR analysis of (a) Ir(III)@m-UiO-66 and (b) Ir(III)@m-UiO-66-NH_2 before and after catalysis.

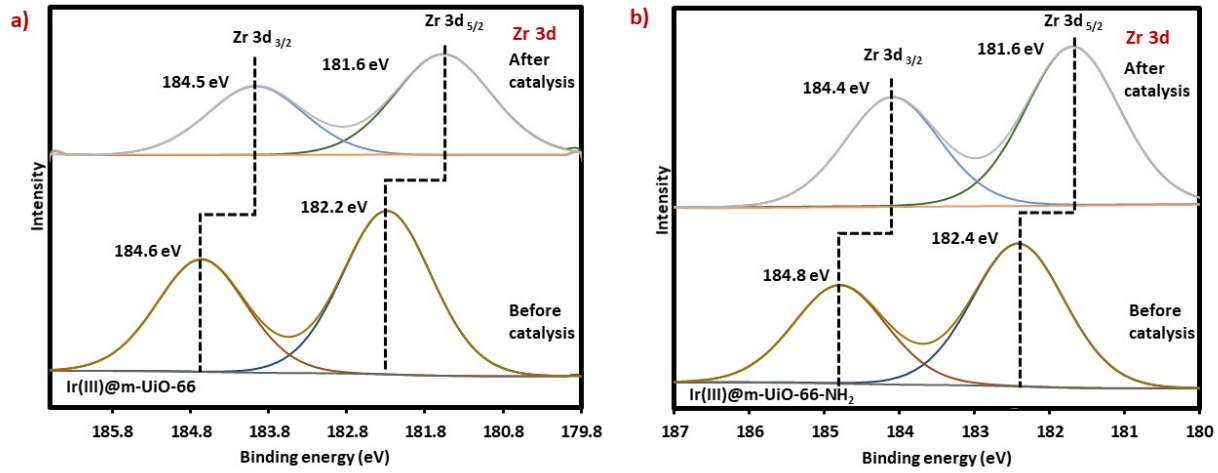

Figure S18. XPS analysis of Zr 3d in, (a) Ir(III)@m-UiO-66 and (b) Ir(III)@m-UiO-66-NH_2 before and after catalysis.

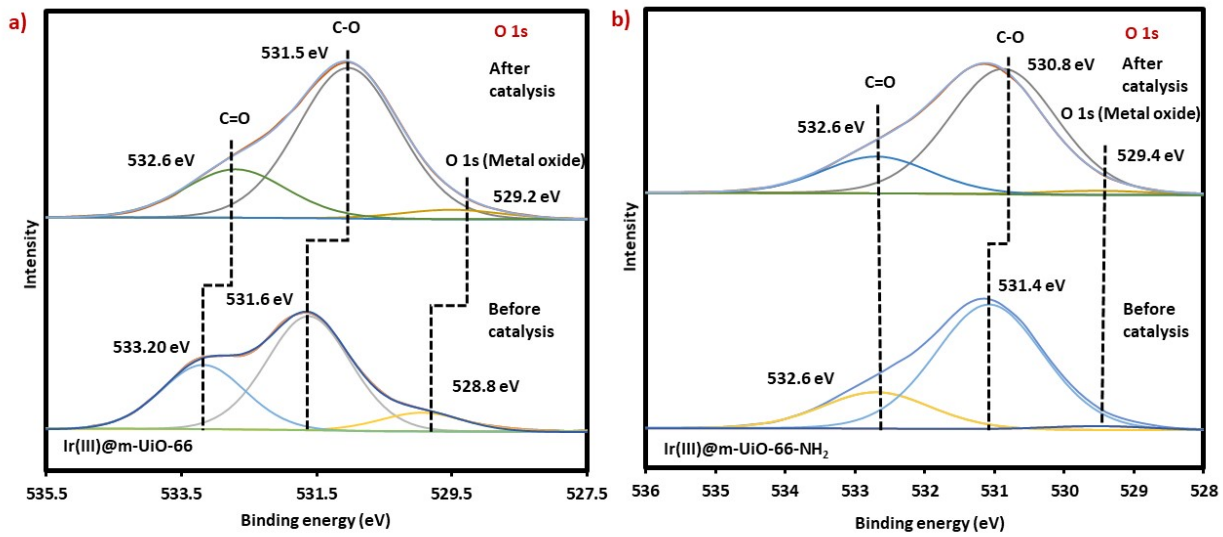

Figure S19. XPS analysis of O 1s in, (a) Ir(III)@m-UiO-66 and (b) Ir(III)@m-UiO-66-NH_2 before and after catalysis.

Table S1: Leaching tests for catalysts

Sample ID	% Ir content	% Zr content
Ir(III)@m-UiO-66	0.0003	0.0001
Ir(III)@m-UiO-66-NH_2	0.0002	0.0001